Anisotropic in-plane properties of (103)/(013) oriented $YBa_2Cu_3O_{7-\delta}$ thin films grown on exact and miscut (110) $SrTiO_3$ substrates

R. P. Campion, P. J. King, K. A. Benedict, R. M. Bowley, P. S. Czerwinka, S. Misat, and S. M. Morley
School of Physics and Astronomy, University of Nottingham, Nottingham NG7 2RD, England
(Received 28 January 1999; revised manuscript received 1 November 1999)

$YBa_2Cu_3O_{7-\delta}$ (YBCO) grows upon (110) oriented $SrTiO_3$ substrates with two equivalent tilt orientations and exhibits regions of each 45° tilt. If the substrate orientation is ''miscut'' from the exact (110) orientation, the two tilts are no longer energetically equivalent, enabling the fabrication of films with controllable tilt disorder. We have carried out a comparative study of (103)/(013) YBCO films deposited onto exact cut (0°) substrates, and onto 3° and 5° miscut substrates where the proportion of minority tilt is about 5% and 2%, respectively. The two-temperature sputter growth process that has been developed yields films which are essentially free of the (110) orientation and which have normal-state resistivities ρ_{001} comparable to ρ_a for a high-quality single crystal. In the superconducting state the three classes of film each exhibit features characteristic of a phase transition for both the [001] and the orthogonal transport current directions. Data from the 0° and 5° films exhibit excellent scaling collapse over very wide ranges of temperature; data from the 3° films scale somewhat less well. Surprisingly, the transition temperatures differ significantly between the two transport directions in the 0° films at all magnetic fields investigated and in the 3° films at higher fields. The nonuniversality of the scaling parameters, the very high values of the exponent *z*, and the dependence of the transition temperature on transport direction cast doubt on a conventional interpretation in terms of a vortex-glass melting transition. Studies of the Ohmic behavior of the 5° films show an in-plane anisotropy which remains constant as the system passes from the normal state, through the superconducting flux flow regime to the Ohmic thermally activated flux creep region. This constancy is consistent with the anisotropy in the vortex damping being equal to the normal-state anisotropy.

I. INTRODUCTION

The high-temperature superconductors may exhibit appreciable dissipation in response to a transport current due to the relatively weak pinning of the fundamental excitations of the system, the vortices associated with the quantization of magnetic flux.[1,2] The vortex movement and thus the voltage are determined by the response of the system to the Lorentz force imposed by the transport current in the presence of intervortex repulsion, vortex pinning, and thermal fluctuations. Although many features of the dissipation are understood, there are still areas of major concern. These include the nature of the phase-transition-like behavior which occurs at temperatures just below regions of flux flow (FF),[3] thermally assisted flux flow (TAFF),[4] and thermally activated flux creep (TAFC).[5] This behavior has been widely attributed to a continuous phase transition between a vortex liquid and a vortex glass phase[6,7] and many authors have reported that data from this region scale under algorithms appropriate to such a transition.[8–12] Nevertheless, concerns have been expressed that the size and nonuniversality of the scaling exponents indicate that such a model does not fully describe the situation.[13–18]

It is particularly interesting to study vortex dynamics in thin films which have considerable in-plane anisotropy since the transport current direction may be varied while keeping the defect structure and mean density and direction of the vortices constant.[18] The preferred growth of the cuprate superconductors along the *a* and *b* directions rather than along the *c* direction[19] ensures that many types of in-plane anisotropic films are relatively difficult to fabricate compared with *c*-axis normal films.[20,21] They often present challenges associated with contacting, aging, and crack formation upon thermal cycling.[22] $Yba_2Cu_3O_{7-\delta}$ (YBCO) thin films with (103)/(013) orientation [i.e., films whose (103) or (013) planes lie parallel to the sample surface] may be grown reproducibly upon (110) cut $SrTiO_3$ or $LaAlO_3$ substrates by carefully controlling the substrate temperature during growth.[23–25] Such films offer very low normal-state resistivities together with substantial in-plane anisotropy both in the normal and in the superconducting states.[26]

At any point within these films the YBCO *c* axis is aligned at 45° to the substrate normal in one of two equivalent orientations [Fig. 1(a)], this leading to the formation of ''tilt domains'' within the film. For accurately cut (110) substrates (where the normal to the cut of the substrate lies in the [110] direction) ''tilt domains'' of either orientation occur with equal probability. A number of researchers have investigated the use of substrates cut with normals tilted away from high-symmetry directions by very small angles (vicinal cuts) or by larger angles (''miscuts'') in order to manipulate growth morphology.[27–29] We use the term ''miscut'' for all angles including vicinal cuts. The use of miscut substrates drastically affects the spiral growth found in *c*-axis normal films,[29–32] and the use of larger angles of miscut can induce substantial in-plane electrical anisotropy and may enhance the critical current by introducing extended defects.[30] Tilting the normal to the cut of $SrTiO_3$ substrates by a few degrees away from the [110] towards the $[1\bar{1}0]$ direction is known to cause the preferential growth of one of the two alternative

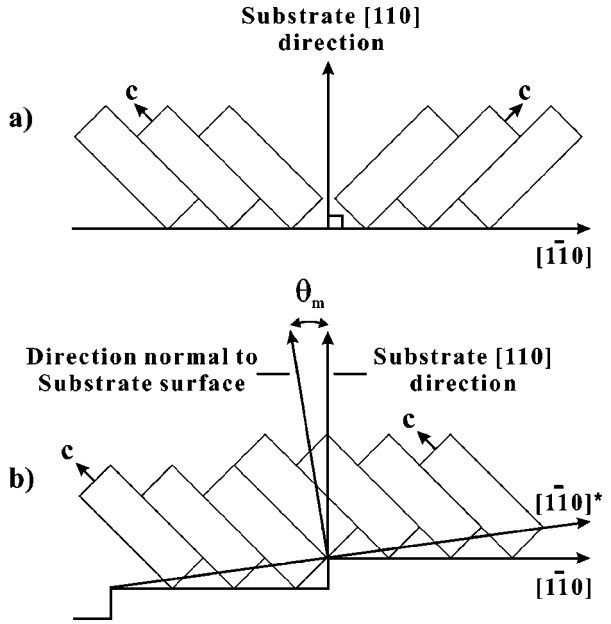

FIG. 1. (a) The two equivalent tilts [(103) and (-103)] of an YBCO film grown upon an exact (110) cut $SrTiO_3$ substrate. The distinction between the (103) and (013) orientations is not shown, the only difference being whether it is the *a* or *b* axis that is perpendicular to the plane of the paper. (b) The use of a substrate ''miscut'' by an angle θ_m leads to one tilt being preferred during growth.

c-axis directions during the fabrication of (103)/(013) YBCO films.[33–36] This is illustrated in Fig. 1(b). This substrate miscut enables control of the tilt disorder, an additional tool in our study.

In the present paper we describe a successful method for the fabrication of high-quality (103)/(013) thin films. We present a detailed comparison of the electrical transport properties of films grown upon exact cut (110) substrates with the properties of films grown upon 3° and 5° miscut substrates. (Throughout this paper a film grown upon, for example, a 3° substrate will be described as a ''3° film.'' The films grown upon 0°, 3°, and 5° miscut substrates will be referred to as the three ''classes'' of film.) We then describe detailed electrical measurements, both for the normal and for the superconducting states, where we observe scaling behavior which is characteristic of a phase transition. The data collapse extremely well onto two scaling curves over very wide ranges of temperature. Our study of the scaling behavior as a function of miscut angle and transport current direction and of the anisotropy of the superconducting behavior raises important questions about the nature of the vortex behavior in these films.

II. FABRICATION OF (103)/(013) THIN FILMS

The heteroepitaxial growth of thin films is controlled by a number of factors which include the substrate film lattice matching, the growth temperature (through such parameters as adatom diffusion lengths), and the adatom supersaturations. While the preferred crystalline orientation of YBCO grown upon(110) $SrTiO_3$ substrates certainly depends upon the substrate temperature via the different lattice matching at different temperatures resulting from differential thermal expansion, the balance is tipped only delicately in favor of the (110) or the (103)/(013) orientations.[23] Since the adatom supersaturations may vary enormously between different preparation methods, it is not surprising that there are variations between the reported optimal growth conditions for (013)/(103) YBCO films and between the orientational purities achieved. Further uncertainty results from possible inaccuracies of several tens of degrees in some reported substrate temperatures that have often not been measured directly.

Terashima *et al.*[23] report amorphous films grown using substrate temperatures below 540 °C. They observe the (110) orientation [i.e., films whose (110) planes lie parallel to the sample surface] for temperatures between 540 °C and 550 °C, a mixture of (110) and (103) between 540 °C and 600 °C, and pure (103) films above 600 °C. Since this report, many authors have used substrate temperatures in the range 720–750 °C for (103)/(013) film growth.[25,33–35] In a more recent and very detailed study by Poelders *et al.*,[36] made on films prepared by a cylindrical magnetron sputtering technique, the substrate temperature has been carefully measured. Poelders *et al.* find amorphous films for growth below 600 °C and pure (110) orientation for temperatures just above this. As increasing substrate temperatures are used the proportion of the (110) orientation steadily declines, but even at 800 °C a (110) volume fraction of about 15% is reported. The (103) orientation is first found at 620 °C, the (103) fraction reaching a broad plateau of about 50% by about 700 °C. By 740 °C appreciable (013) orientation appears. It should be noted that in the work of Poelders *et al.*, which extends to 820 °C, there is no temperature at which the films are free of the (110) orientation.

Our own (103)/(013) YBCO films were grown on (110) $SrTiO_3$ substrates by a self-templating two-temperature method which has been found empirically to give high-quality films with extremely low proportions of the YBCO (110) orientation. They were deposited by 90° off-axis rf magnetron sputtering from a stoichiometric YBCO target. The substrates were mounted using silver paste onto a stainless steel block, which was heated by enclosed quartz halogen projector bulbs. The temperature was sensed by a thermocouple attached to the block; the heater block temperatures (which are quoted) are typically 5 °C higher than the actual substrate temperatures. The growth chamber was filled with a (60% O_2)/(40% Ar) mixture to about 60 mTorr and, just before the film growth process, the substrate was heated to 750 °C for 10 min in this atmosphere. A 10–15 nm YBCO template layer was then grown over 15 min at a temperature of 650 °C. The temperature was then raised to 750 °C at 10 °C/min while growth continued. The remainder of the growth took place at this higher temperature. Following growth, the chamber was flooded with oxygen to atmospheric pressure. The block temperature was then held at 750 °C for 20 min, and then cooled to room temperature at 10 °C per minute. The film quality was finely tuned by modest adjustments to the chamber pressure. While the growth method was optimized using ''exact'' (110) cut substrates, the same growth method was used to fabricate films upon miscut substrates with equal success.

X-ray diffraction (XRD) measurements indicate that the fraction of (110) orientation in films prepared by this method is usually below the limit of delectability ($<1\%$). The vol-

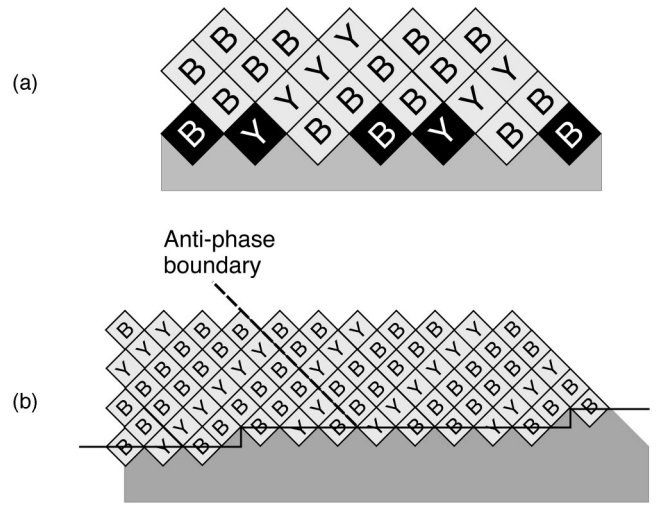

FIG. 2. (a) Growth of tilted YBCO upon a (110) $SrTiO_3$ substrate, noting the need for additional yttrium (Y) or barium (B) cube units which are fractions of the full unit cell in order to avoid massive growth disorder. (b) The structure of miscut substrates showing steps and terraces. Nucleation at a step is preferred. Again cube units are required to avoid a large number of growth defects. In thicker films any residual mismatching will tend to grow out via stacking faults.

ume ratio of the two tilts has been determined from the corresponding XRD lines.

Following XRD and microscopic examination, the films were patterned by wet lithography and silver contacts deposited by thermal evaporation. Usually the tracks were 50 μm wide and 5000 μm long between the pair of voltage contacts. Electrical measurements on films grown upon exact cut substrates have been made on long tracks oriented along the substrate [001] and [110] directions. In the case of miscut substrates, measurements have been made along the [001] and along the orthogonal direction which we will refer to as the [110]* direction, for convenience, even though this direction differs from the [110] direction by the small angle of miscut.

III. MICROSTRUCTURE OF (103)/(013) YBCO THIN FILMS

Consideration of how (103)/(013) YBCO of either tilt nucleates and grows upon a (110) $SrTiO_3$ substrate leads to the conclusion that yttrium and barium cube subunits are required at the substrate surface in addition to full unit cells. This is shown in Fig. 2(a). Where this does not occur an antiphase boundary will be generated which may grow out as the film thickens via stacking faults, which are known to occur readily in YBCO. Eom *et al.*[25] and Marshall and Eom[37] have carried out transmission electron microscopy (TEM) and scanning electron microscopy (SEM) investigations of the microstructure of the later growth. They report that initial nucleation of very many grains of either tilt is followed by rapid growth along the *ab* planes, leading to the formation of large numbers of triangular grains separated by either basal plane faced tilt boundaries or by symmetric or almost symmetric tilt boundaries. Thus the first 5 nm or so of the thickness of a film consists of very many small grains.

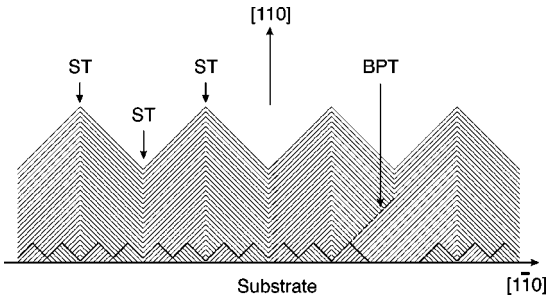

FIG. 3. Simplified structure of a (103) YBCO film grown upon an exact cut (110) $SrTiO_3$ substrates. The lines schematically represent the superconducting copper-oxygen planes. BPT, basal plane tilt boundary; ST, symmetric tilt boundary.

(In our own films these triangular grains should be very fine due to the relatively low temperature of nucleation.) Since the *ab* planes are no longer exposed, further growth occurs predominantly along the *c* axis, and far larger grains of both tilts develop. These are referred to as ''tilt domains.'' The boundaries between domains of opposite tilt are either basal plane faced tilt boundaries or symmetric (or almost symmetric) tilt boundaries, the latter dominating in thicker films as studies by Guilloux-Viry *et al.*[33] and by Rossel *et al.*[34] confirm. These features are illustrated in Fig. 3.

As Fig. 3 shows, the dominance of symmetric tilt boundaries will lead to tilt domains of about equal width along the [1$\bar{1}$0] direction. This is evident in the observed surface structure, which has a topology illustrated as being similar to that of a rustic brick wall, an individual ''brick,'' a tilt domain, being approximately rectangular in shape, and typically about 5 times longer in the [001] direction than in the [1$\bar{1}$0] direction.[25,37] The simplified illustration of Fig. 3 also suggests that the domains will be of alternate tilt along the [1$\bar{1}$0] direction. However, a more detailed examination of the actual domain shapes shows that, while they are certainly elongated in the [001] direction, the shapes are intermeshed and closer to irregular rice grains than to rectangles. Figure 4(a) shows an atomic force microscope (AFM) picture of a (103)/(013) film of average thickness 125 nm grown upon a nominally exact cut (110) substrate, the display being a ''three-dimensional'' representation viewed as if from above. The domain structure is quite evident from the thickness variations. The tilt domains are elongated in the [001] direction, being on average about 0.5–0.8 μm long and 0.1–0.2 μm wide at the surface. The rms variation in thickness of the film is 9 nm, with variations of twice that amount being uncommon. Only occasional secondary phases may be observed at the boundaries between domains. The form of the domain intermeshing and consideration of the tiling of a plane with shapes of two types indicates that the tilt anticorrelation along the [1$\bar{1}$0] cannot be complete, while tilt correlation along the [001] direction must be weak. The degree of correlation in the [001] direction is important in the interpretation of the normal-state resistive anisotropy of these films.[38]

In this structure domains of opposite tilt are connected along the [001] direction by 90° twist boundaries, and in the [1$\bar{1}$0] direction by basal plane tilt boundaries or more commonly by symmetric or almost symmetric tilt boundaries.[25,37] These boundaries are illustrated in Fig. 3. The superconduct-

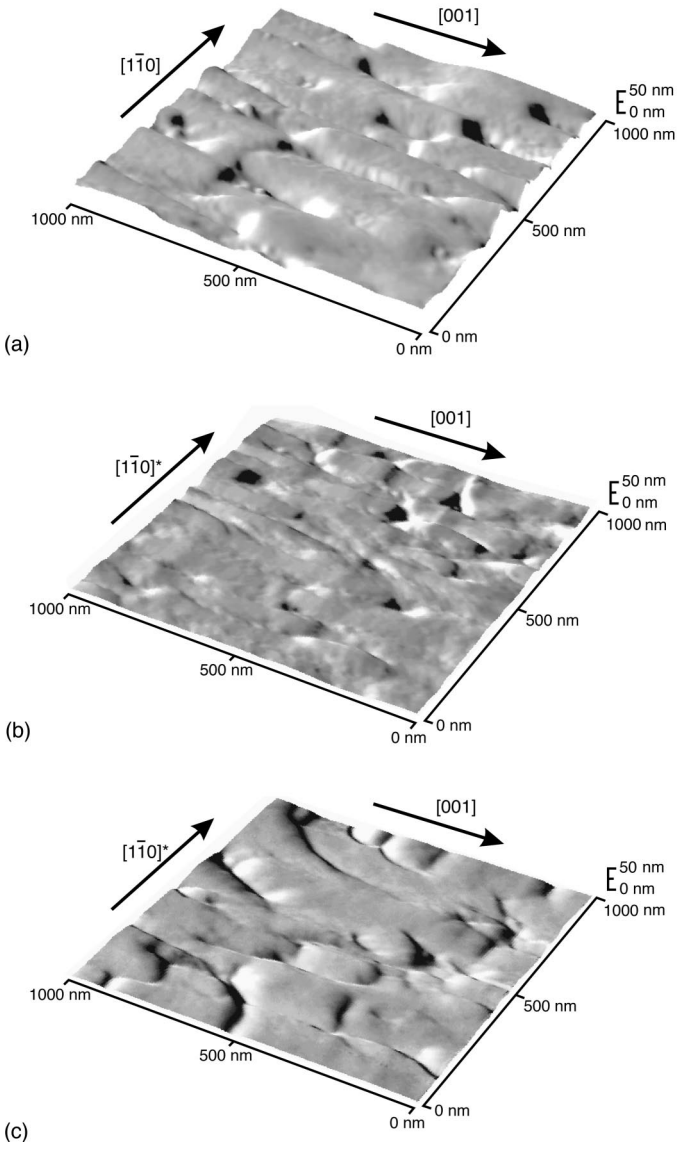

FIG. 4. AFM images of the surfaces of typical films. (a) A film grown upon an exact cut substrate. (b) A film grown upon a 3° miscut substrate. (c) A film grown upon a 5° miscut substrate. In each case the [001] and [1$\bar{1}$0]* directions are indicated.

ing order parameter is now known to have a predominantly *d*-wave nature. Here 90° twist boundaries provide lobe matching and no severe disruption of the superconducting properties, while tilt boundaries provide mismatching and severe disruption.[38,39] Further disruption at tilt boundaries may be provided by crystallites of secondary phases, which are preferentially found at these sites. Tilting the cut of $SrTiO_3$ substrates by a few degrees away from the [110] towards the [1$\bar{1}$0] direction causes the preferential growth of domains with one of the two alternative *c*-axis directions; the two tilts are no longer energetically equivalent.[33–35] Even though XRD and TEM studies confirm the dominance of one tilt in films miscut by only a few degrees, little has been published concerning the first or subsequent stages of growth immediately following nucleation. The effect of tilting the normal to the substrate cut away from the (110) direction will be to introduce steps and terraces; see Fig. 2(b). The mean step height to terrace spacing corresponds to the miscut angle. The terrace spacing will normally be somewhat irregular following polishing. It has been reported that the atomic mobility which occurs during a high-temperature anneal induces regular terrace spacing,[30,31] but in our own work we have not approached the temperature at which this is likely to occur (950 °C) and the terracing will be less regular. The growth of YBCO films on a miscut substrate will be determined by competing nucleation at steps and on the terraces, this depending upon the different adatom diffusion lengths at the growth temperature. Since a 3° miscut certainly induces a preferred tilt in (103)/(013) films, it follows that nucleation is strongly preferred at the steps and that the diffusion lengths must be greater than the mean terrace width, about 8 nm for 3° films. The growth of relatively defect-free films again relies on the existence of partial unit cell cube units at the interface. However, it may be seen from Fig. 2(b) that, even then an antiphase boundary will be generated if the number of cells across a terrace is not divisible by 3. These antiphase boundaries may grow out via stacking faults as the film thickens.

Our own studies show that films grow on miscut substrates at much the same rate as on exact cut substrates for similar sputtering conditions. Figure 4(b) shown the equivalent AFM representation of a 130-nm-thick film grown upon a 3° miscut substrate. XRD studies show that this film has a volume tilt ratio of 95%:5%; any (110) phase exists at a level well below 1%. Surface structure which appears to correspond to ''domainlike'' growth areas is evident but the more or less regular domain arrangements of the films grown upon exact cut substrates reported by Eom *et al.*[25] and others [and evident in Fig. 4(a)] are not present. In particular large areas of the film are connected relatively smoothly with only weak discontinuities where ''domains'' meet. The film clearly shows a defect structure where growth areas meet, but we are unable to identify which areas correspond to the 5% minority tilt. The films are generally far smoother than those grown upon exact cut substrates; the rms variation in thickness is typically 3 nm, a factor of 3 less than for exact cut substrates.

Figure 4(c) shows the AFM representation of a typical film grown upon a 5° miscut substrate. In this film XRD and transport measurements indicate that the fraction of the minority tilt is about 2%; no (110) phase is detected at the 1% level. The surface topology is somewhat similar to that of the 3° film shown in Fig. 4(b). The surface features produced by the merging of the different growth areas are again shallower than for the films on exact cut substrates and many ''domains'' join relatively smoothly with small surface disturbances. The rms variation in thickness is 3 nm, similar to that of the 3° film.

In films where one tilt dominates, nucleation will generally not be followed by the development of triangular grains, followed then by the growth of larger domains. However, a film mainly of one tilt with small areas of the other, the two being separated by symmetric tilt boundaries, does not provide sufficient release for the stress induced by the $SrTiO_3$/YBCO lattice mismatch except in the case of very thin films. Whether this release is caused via the numerous stacking faults originating at the substrate/YBCO interface is not clear; nor has the development of the antiphase boundaries been studied in this system. Nevertheless, the surface

indications of many distinct growth areas in (103)/(013) films grown upon miscut substrate are evidence for the presence of numerous internal defects which need to be characterized so that their effect on the transport properties can be ascertained. More work on the microstructure of these films is necessary.

In summary, the films grown upon exact cut substrates show the expected tilt domain structure with pronounced surface features where domains join. The films on 3° and 5° miscut substrates also show considerable, but much less regular, surface structure together with much shallower features where growth areas join. On average these films are ''smoother'' by a factor of 3. No cracks have been seen in the films studied.

IV. ELECTRICAL MEASUREMENT TECHNIQUES

Cryogenic measurements of $R(T)$ and of various I-V-B-T characteristics were made by conventional four-probe measurements under computer control using an Oxford Instruments helium gas flow cryostat. The dc voltages were sensed using an EM Electronics A10 sub-nanovolt low-noise amplifier; at each measurement the current direction was reversed to ensure consistency. The error in the measurement of the voltage was better than 1% over the whole range reported here plus a random error of 1–2 nV. ''Zero-field'' measurements were made with the cryostat tail and sample screened by a double mu-metal shield, reducing the Earth's field by a factor of 5000. Magnetic fields were applied perpendicular to the substrate surface in all cases. All measurements in the superconducting state were made by applying the magnetic field at or above T_c and then cooling to the temperature of measurement.

V. COMPARATIVE NORMAL STATE BEHAVIOR

By comparing the normal-state properties of films grown upon exact cut and upon 3° and 5° miscut substrates a very consistent picture emerges. Figure 5 shows the resistivity $\rho(T)$ as a function of temperature T for one film of each class and for current flow both in the [001] and in the $[1\bar{1}0]^*$ directions. Table I provides numerical data both for these films and for one further 3° and 5° film. The values of $\rho_{[001]}$ are not only remarkably consistent between the three classes of film, but are comparable in magnitude with the resistivity of a very-high-quality YBCO single crystal. It may be seen that $\rho_{[001]}$ extrapolates close to the origin in each case, as would also be found in a well-oxygenated single crystal. Friedmann *et al.*[40] quote values for $\rho_a(100\ \mathrm{K})$ of 40 and 53 $\mu\Omega$ cm, and for $\rho_b(100\ \mathrm{K})$ of 21 and 25 $\mu\Omega$ cm at 100 K for well-oxygenated samples; our own range of 37–50 $\mu\Omega$ cm is comparable to the values for ρ_a. Agreement with the single-crystal values for ρ_a rather than for ρ_b may be due to both the dominance of (103) over the (013) orientation and to some twinning which disrupts the copper oxygen chains which are responsible for the lower ρ_b resistivity. Since in the case of films on exact cut substrates [001] transport must involve 90° twist boundaries, whereas twist boundaries are not involved in [001] transport for the miscut films, the consistency of ρ_{001} between the classes of film is an indication of the very small impediment

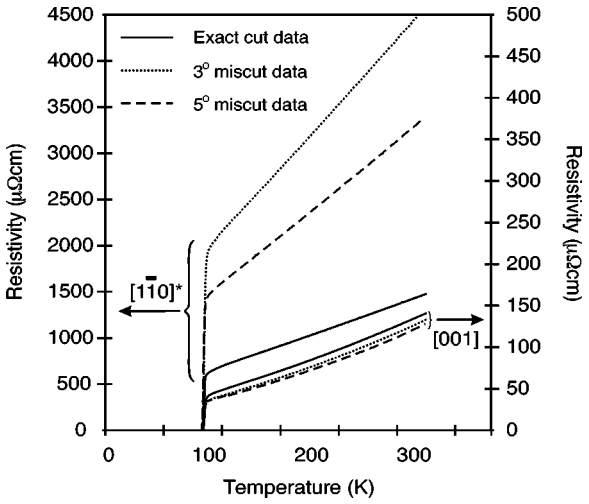

FIG. 5. Resistivity plotted against temperature for current flow along the [001] direction and the $[1\bar{1}0]^*$ direction. Film 32 grown upon an exact cut substrate, solid lines; film 40 grown upon a 3° miscut substrate, dashed lines; film 41 grown upon a 5° miscut substrate, dotted lines. Measurements were made using a transport current of 1 μA. Each film was about 130 nm thick.

imposed by twist boundaries in the normal state.

The data for $\rho_{[1\bar{1}0]^*}$ extrapolate less close to the origin, $\rho(0\ \mathrm{K})/(\rho 100\ \mathrm{K})$ being consistently close to 0.35 except for the occasional sample thought to be less well oxygenated (see Table I). The anisotropy ratio $\rho_{[1\bar{1}0]^*}/\rho_{[001]}$ at 100 K is, however, dramatically different when we compare the exact cut samples to the samples grown upon miscut substrates. The anisotropies of films grown upon exact cut substrates by the technique described lie in the range 14–25, generally toward the lower end of this range, depending upon the details of the growth conditions. In contrast it may be seen from Table I that the anisotropies of the typical 3° films are 45.5 and 51.5 at 100 K, while the equivalent numbers for the 5° films are 40 and 48.

Fletcher *et al.*[41] have pointed out that current may flow in helical paths along a 90° twist boundary by ab-plane conduction alone. Campion *et al.*[38] have used this mechanism to propose that in the domained films which occur upon exact cut substrates $[1\bar{1}0]$ transport occurs by forward flow along the twist boundaries and sideways flow across ab planes, thus avoiding the tilt boundaries, which are expected to contribute considerable impediment to flow. Campion *et al.* have been able to make a crude estimate of the normal-state anisotropy by estimating the effective length of the tortuous current paths involved on the plausible assumption that the domain tilts are uncorrelated in the [001] direction. They estimate anisotropies in the range 10–20, consistent with our finding. For films grown upon miscut substrates, such that one tilt occurs with a very low fraction, the current paths of Campion *et al.* become very long and the shunting c-axis conduction dominates.[38] The observed in-plane anisotropy may then be deduced from the resistivity for a single crystal tilted by 45° with respect to the [110] crystallographic axis of the substrate: $\rho=\rho_{ab}\sin^2(45°+\theta_m)+\rho_c\cos^2(45°+\theta_m)$ where θ_m is the miscut angle, and ρ_{ab} is a suitable ''average'' of ρ_a and ρ_b. In the light of our ρ_{001} values we will use $\rho_{ab}=\rho_a$, and $\rho_c/\rho_{ac}=120$ (see Friedmann *et al.*[40]). The

TABLE I. Normal-state behavior.

Film No.	Angle	T_c (Mid)	$\rho_{[001]}(100\ \mathrm{K})$ ($\mu\Omega$ cm)	$\rho_{[1\bar{1}0]*}(100\ \mathrm{K})$ ($\mu\Omega$ cm)	$\frac{\rho_{[1\bar{1}0]*}(0\ \mathrm{K})}{\rho_{[1\bar{1}0]*}(100\ \mathrm{K})}$	Anistropy
32	0°	85.2	48	690	0.35	14.4
34	3°	84.3	48	2200	0.7	45.8
40	3°	85.0	42	2200	0.37	51.5
41	5°	84.5	40	1600	0.32	40.0
42	5°	84.6	43	2100	0.35	48.0

predicted anisotropy is then 54 for the $\theta_m = 3°$ and 49 for $\theta_m = 5°$. These estimates are in good agreement with our findings given in Table I.

VI. BEHAVIOR IN THE SUPERCONDUCTING STATE

Detailed superconducting-state *I-V* measurements have been made in a range of magnetic fields for both the [001] and the $[1\bar{1}0]^*$ transport directions. A typical family of current voltage curves for a range of fixed temperatures is illustrated in Fig. 6; in the figure the temperature reduces from left to right. The different regions of behavior include Ohmic behavior (O) found over a range of temperatures below T_c, and nonlinear behavior (N), found at lower temperatures and higher currents. At one particular temperature, which we call T_t, the curvature of the log(*I*)-log(*V*) characteristics changes discontinuously from positive, through straight line behavior, to negative. We will show that the data scale over a wide region about the ''transition temperature'' T_t, and then consider the anisotropy in the Ohmic region above T_t and in the region below T_t, where the data show critical current behavior.

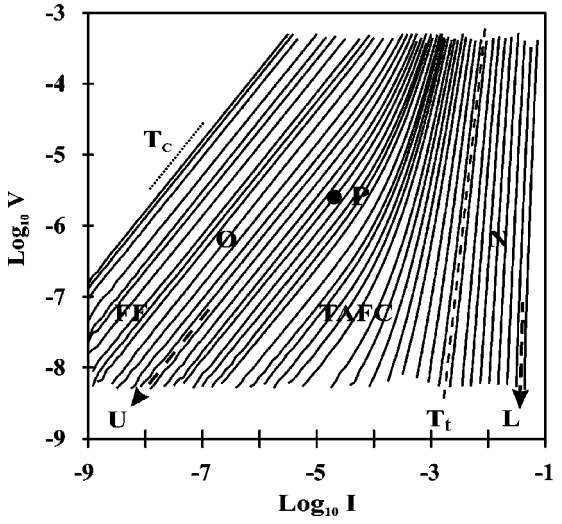

FIG. 6. An illustrative family of current-voltage curves taken at various fixed temperatures, presented on logarithmic scales. The data were taken on film 34, for transport in the [001] direction, in a perpendicular magnetic field of 0.6 T. T_c, the region of Ohmic behavior (O), the phase transition temperature (T_t), and the low-temperature, nonlinear regime (N) are indicated. The point P indicates a typical ''bias'' point for angular studies, while U and L indicate typical upper and lower limits of the region for which excellent scaling is obtained.

A. Theoretical ideas

In the high-temperature superconductors the dissipation results from the motion of vortices, the dynamics being determined by the interplay of vortex-vortex interactions, vortex-pin interactions, the Lorentz forces induced by the transport current, thermal fluctuations, and viscous damping.[1,2] As yet no complete theory exists for this complex system which would enable the overall form of current-voltage characteristics, such as those of Fig. 6, to be qualitatively related to the physical properties of the sample. However, many of the elements of such a theory are now in place, enabling some interpretation of the data. At temperatures not far below T_c is a region of Ohmic behavior where viscous damping dominates the effects of pinning, a region often described as the ''flux flow'' regime (FF in Fig. 6).[3] As the temperature is lowered pinning plays an increasingly important role. At first pinning impedes flux flow, which is, however, assisted by thermal excitations. This behavior is described as thermally assisted flux flow.[4] At yet lower temperatures the effect of pinning is sufficiently large that flux movement would not proceed without thermal activation. The Anderson-Kim analysis of thermally activated flux creep predicts Ohmic behavior at low currents, with the ratio V/I increasing exponentially with current at higher currents. Experimentally, however, power law rather than exponential behavior is almost invariably observed. The simple Anderson-Kim expression has been modified to produce power law behavior by introducing barrier heights dependent upon current as $\ln(I_0/I)$, where I_0 is a temperature-dependent constant.[1,42]

Experimentally the temperature dependence of the Ohmic resistivity predicted by Anderson and Kim for thermally activated flux creep is often found over limited ranges of temperature; it is sometimes not seen at all. Usually, the low-current Ohmic resistivity plummets increasingly rapidly as a ''transition temperature'' is approached from above; the curvature of the current-voltage characteristics changes from being positive above the transition temperature to being negative below. Power law behavior is found at the transition temperature itself. These features may be found in the data of Fig. 6, where the transition temperature is marked as T_t. The transition temperature separates a higher-temperature region, in which dissipation occurs at arbitrarily small currents, from a lower-temperature region in which there is an abrupt onset of dissipation at a critical current whose value depends upon temperature.

These features have been attributed to a continuous thermodynamic phase transition at which the system passes from a vortex liquid to a vortex glass (VG),[6,7] a phenomenon ex-

TABLE II. Scaling parameters obtained by collapsing the I-V data for 0° film 24 on the basis that $d=3$. H refers to transport along the $[1\bar{1}0]$* direction while L refers to transport along the [001] direction.

Field (T)	ν	z	T_t (K)	T_+	T_-	Class of fit
0.0 L	1.11	8.4	83.58	84.1	82.3	B
0.03 L	1.24	9.9	82.00	84.0	80.3	A
0.1 L	1.26	10.0	81.30	83.6	79.1	A
0.3 L	1.28	10.3	80.28	83.0	78.1	A
1.0 L	1.22	10.7	78.50	82.1	73.2	A
0.0 H	1.23	9.2	82.70	83.7	79.7	B
0.03 H	1.24	11.6	80.57	83.1	78.4	A
0.1 H	1.36	11.7	79.48	82.6	75.8	A
0.3 H	1.36	12.5	78.00	81.6	74.2	A
1.0 H	1.38	12.6	75.55	81.2	65.5	A

pected in systems with considerable point disorder. Many authors have since demonstrated that dc and ac response data from superconducting single crystals and *c*-axis normal thin films obeys the class of scaling expected on general grounds if the physical processes leading to the transition are dependent on a single scale length and a single time scale.[7,43–46]

However, the existence of scaling does not, by itself, prove beyond doubt that there is a thermodynamic phase transition; nor does it lead directly to an understanding of the mathematical form of the two functions onto which the data collapse under scaling.[8,13,47–50]

B. Scaling behavior

At a continuous thermodynamic phase transition the correlation length ξ and the correlation time τ both diverge in the critical region. Many authors have supposed that such length and time scales govern the dynamics of vortices and that near the phase transition these divergent scales are the only relevant parameters.[6,7] By constructing appropriate dimensionless numbers an algorithm may be devised for scaling all of the data onto a pair of curves, one for temperatures above the transition, the other for temperatures below. The vector potential **A** has the dimensions of an inverse length, and so the electric field **E** ($\propto \partial \mathbf{A}/\partial t$) can be expressed in terms of the dimensionless parameter $E\xi\tau$. The current density **j** is proportional to $\partial f/\partial \mathbf{A}$, where f is the Ginzburg-Landau free energy density. Hence $j\xi^{1-d}$ is a dimensionless parameter. In d dimensions we expect

$$E\xi\tau = F_{\pm}(j\xi^{1-d}, B\xi^2),$$

where $F_+(x)$ is the scaling function for temperatures above T_t, $F_-(x)$ is the scaling function for temperatures below T_t, and B is the magnitude of the magnetic induction field. Near T_t the correlation length is expected to diverge as $|T-T_t|^{-\nu}$ and the correlation time to diverge as $|T-T_t|^{-z\nu}$, where z and ν are critical exponents. If the length scale associated with B can be ignored, the data are expected to scale as[6,7]

$$E|T-T_t|^{-\nu(z+1)} = F_{\pm}(j|T-T_t|^{-\nu(d-1)}).$$

The functions $F_+(x)$ and $F_-(x)$ approach each other for large x, each asymptotically assuming the form of a power law of gradient $(z+1)/(d-1)$. For temperatures above T_t the behavior becomes Ohmic for small x, that is, $F_+(x) \propto x$ for small x.

In practice we measure the voltage drop V over a length l ($V=El$) and the current I through a cross-sectional area S ($I=jS$). It is better to consider the scaling of V/I versus I since the Ohmic behavior found at higher temperatures and low currents simplifies the scaling procedures. The relationship between V/I and I is described by

$$\frac{(SV/Il)}{|T-T_t|^{\nu(z-d+2)}} = G_{\pm}\left(\frac{I}{S|T-T_t|^{\nu(d-1)}}\right).$$

In practice we use the logarithm of this equation and the parameter $\log(S/l)$ appears as an irrelevant constant, as does $\log(S)$. (The area S and the length l allow the generation of other dimensionless ratios involving the correlation length. It is explicitly assumed in the analysis that such parameters as l/ξ and S/ξ^2 are irrelevant in the scaling function.) To test whether the $\log(V/I)$ versus $\log(I)$ curves for fixed temperatures exhibit scaling properties, individual curves are shifted onto a master curve by simple displacements along the $\log(V/I)$ and $\log(I)$ axes. The $\log(V/I)$ versus $\log(I)$ isotherms taken above T_t scale onto the master function G_+, while the $\log(V/I)$ versus $\log(I)$ isotherms taken below T_t scale onto the second master function G_- *using exactly the same scaling parameters z and* ν. The scaling is only predicted over the range of temperatures for which the time and length scales vary as an inverse power of $|T-T_t|$. The two functions G_+ and G_- approach each other at T_t, each asymptotically assuming the form of a power law of gradient $(z-d+2)/(d-1)$.

We have analyzed the extent to which data for our three classes of film collapse under scaling using software which appropriately scales $\log(V/I)$ versus $\log(I)$ curves in response to chosen values of T_t, and z. T_t is initially selected within the narrow range of temperature for which the current-voltage characteristics have behavior closest to power law. ν and z are then adjusted to produce the most satisfactory scaling both above and below T_t. T_t is then adjusted by very small amounts to see whether any overall improvement can be obtained, aided by a zoom facility in the computer software. The resulting fitting parameters for a 0°, a 3°, and a 5° film are shown in Tables II, III, and IV, z and ν being

TABLE III. Scaling parameters obtained by collapsing the *I-V* data for 3° film 34 on the basis that $d=3$. H refers to transport along the $[1\bar{1}0]$* direction while L refers to transport along the [001] direction.

Field (T)	ν	z	T_t (K)	T_+	T_-	Class of fit
0.0 L	-	-	-	-	-	C
0.01 L	1.40	5.5	81.00	81.8	79.7	B
0.03 L	1.45	8.3	80.18	81.7	78.1	B
0.1 L	1.52	9.5	79.35	81.5	77.1	A/B
0.3 L	1.45	10.0	78.30	81.5	74.2	A
0.6 L	1.33	9.7	77.10	81.0	71.3	A
0.0 H	–	–	–	–	–	C
0.01 H	1.35	8.5	80.70	81.7	77.5	B
0.03 H	1.26	10.5	79.66	81.5	75.7	A
0.1 H	1.31	11.0	78.60	80.4	73.9	A
0.3 H	1.45	12.8	77.25	80.7	72.3	A
0.6 H	1.45	12.8	75.70	80.3	68.5	A

quoted assuming $d=3$. In general the quality of collapse worsens appreciably if data from temperatures above an upper limit T_+ and below a lower limit T_- are used; the values T_+ and T_- which have been used are also given in the tables. Typical upper and lower limits of the temperature range for which we have scaled the data are indicated in Fig. 6 by *U* and *L*.

Much of the data scale excellently over surprisingly wide ranges of temperature. The excellence of the better scaling collapses may be seen from Fig. 7 which presents data from film 24 taken at a magnetic field of 0.3 T and with a current direction of [001]. The remarkable quality of the scaling is evident from the expansions to the right of the main diagram which show that the spread of the $\log_{10}(V/I)$ data is on the scale of 0.1–0.2 % of the overall logarithmic voltage range, that is, about 25. (An appreciable fraction of this spread can be attributed to the small temperature drifts which occur during the measurements of a single *I-V* curve. The spread results from the fact that during the scaling, each data point has been assigned the mean temperature of the set rather than the actual temperature at which each point was measured. Thus Fig. 7 underestimates the true accuracy to which the data scales.) The quality of the scaling collapse for each film and magnetic field is indicated in the tables by a letter: ''A'' indicates that the data from the specified temperature range collapse onto the two master curves very well indeed with a spread of less than 0.5% of the overall logarithmic voltage range; ''B'' indicates somewhat poorer scaling, the spread of data being up to 1.5% of the overall logarithmic voltage range. In the case of ''C'' the individual lines are distorted from the form that would make good scaling possible: there is, for example, no temperature at which good power law behavior is displayed. Where the data scale to the quality we have described as ''A'' it is generally possible to determine T_t to ± 0.15 K, ν to ± 0.05, and z to ± 1.0 at low fields, the corresponding figures at fields of 1 T being ± 0.3 K, ± 0.3 K, ± 0.1, *and* ± 1.2. *Where the letter C occurs in the table no scaling parameters are given.*

In general the data taken in low fields scale somewhat less well. However, for the 0° films the scaling is excellent once the applied field exceeds 0.02 T. It may be seen from Table II that ν lies in the range 1.2–1.4 for both transport directions, while z is close to 10 for the [001] direction and 12 for the $[1\bar{1}0]$ direction. In each case there is a slight but significant increase in z with increasing magnetic field. T_t falls smoothly as the magnetic field is increased. While the data for the 3° films scale better at higher fields, the scaling is relatively poor compared with that for the 0° films, particularly for [001] transport (Table III). Only at higher fields is

TABLE IV. Scaling parameters obtained by collapsing the *I-V* data for 5° film 41 on the basis that $d=3$. H refers to transport along the $[1\bar{1}0]$* direction while L refers to transport along the [001] direction.

Field (T)	ν	z	T_t (K)	T_+	T_-	Class of fit
0.0 L	1.13	8.1	81.80	82.4	79.6	B
0.03 L	1.02	12.5	80.50	82.3	74.7	A
0.1 L	1.12	14.8	79.20	81.7	73.7	A
0.3 L	1.20	14.4	77.70	80.8	71.9	A
1.0 L	1.21	13.3	74.90	79.6	64.7	A
0.0 H	1.40	7.7	81.70	82.1	80.6	B
0.03 H	1.45	8.0	80.70	81.7	80.1	A
0.1 H	1.65	8.5	79.50	81.5	76.4	A
0.3 H	1.65	10.6	77.90	80.7	75.2	A
1.0 H	1.35	12.0	74.70	78.5	68.7	A

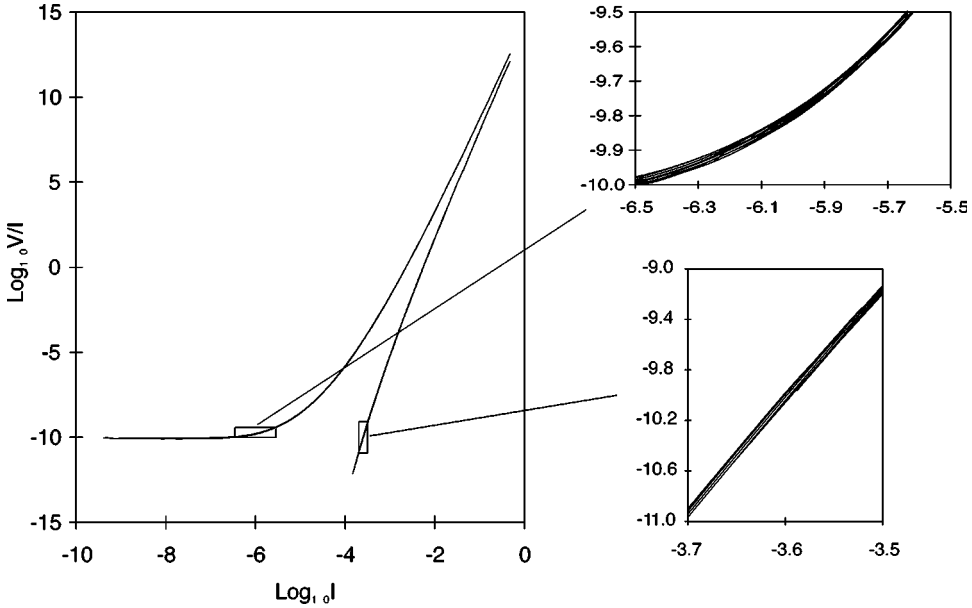

FIG. 7. The left hand diagram shows the overall scaling collapse obtained for the data of sample 24 taken in a magnetic field of 0.3 T. Data below 10 nV are not included. The diagram encompasses 25 decades of voltage and over 8 decades of current. The two rectangular areas are shown expanded to the right. For the areas within the boxes the collapsed data lie within a range of 0.13% of the overall logarithmic voltage range above T_t and within a range of 0.25% below T_t.

excellent scaling obtained. In the nonlinear regime the individual I-V curves show a tendency towards Ohmic behavior at lower voltages than occurs for the 0° or 5° films, and we have removed some of the higher-voltage data from the scaling. Over the range of fields for which the scaling parameters are quoted, ν lies in the range 1.2–1.5 for both transport directions, while z shows a tendency to increase with magnetic field, lying in the range 8–10 for the [001] direction and 10–13 for the $[1\bar{1}0]^*$ direction once the field is large enough to ensure excellent scaling. Again T_t falls smoothly with increasing magnetic field.

The data for the 5° films scale very well indeed except at fields below 0.03 T. ν lies in the range 1.0–1.2 for the [001] transport direction and 1.3–1.65 for the $[1\bar{1}0]^*$ direction, while the corresponding z ranges are 13–15 and 8–12 over the field range in which good scaling is found (Table IV). Again T_t falls increasingly rapidly as the magnetic field is raised.

The behavior of T_t for the two transport directions is shown in Fig. 8 as a function of magnetic fields between 0.01 T and 1 T. The solid lines are fits to all the data, including data for fields below 0.01 T, using the function form $T_t(B) = T_t(0)/(1+\alpha B^{\beta})$. The resulting fitting parameters α, β, and the zero-field values of T_t are given in Table V. For the 5° film, the transition temperatures for the two transport directions are the same to within the experimental error. $T_t(0)$ lies about 2.8 K below T_c in each case. The exponent $\beta = 0.51 \pm 0.05$. For the 3° film appreciable differences between the values of T_t are observed for the two transport directions, differences which at higher fields lie clearly outside the experimental error. The difference, however, is insignificant at zero magnetic field, the $T_t(0)$ values lying just over 2 K below T_c. The β value is 0.36 ± 0.04. For the 0° film the values for the two directions are similar at 0.36 ± 0.04. However, the difference between the T_t values for the two transport directions is very marked [Fig. 8(a)], lying well outside any experimental error. Even at zero field the two $T_t(0)$ values 83.6 K ([001]) and 82.7 K ($[1\bar{1}0]^*$) are clearly distinct.

C. Comparative behavior in the Ohmic regime

For domained films it has been previously reported that when the magnetic field is rotated in the plane containing the [110] and $[1\bar{1}0]$ directions the Ohmic resistance exhibits maxima at angles corresponding to the field being aligned with the c axis of either tilt.[24] In measurements close to region P of Fig. 6 we confirm two almost equal maxima. When such measurements are repeated on 3° and 5° films, however, only a single peak is found, confirming that the dissipation is controlled by one tilt alone, the tilt shown in Fig. 1(b).

Figure 9 shows the Ohmic resistivity for the ''exact cut'' film 24 as a function of temperature, both in zero field and in a field of 1 T, plotted in Arrhenius form as $\log_{10}(\rho)$ versus $1/T$. Data for perpendicular fields of 0.03, 0.1, and 0.3 T were also obtained, the results lying smoothly between the curves shown in Fig. 9. This data cover the normal state above T_c, the fluctuation regime close to T_c, the flux flow regime below T_c, and the lower-temperature region where thermally activated flux creep occurs.

Our data indicate the presence of a phase transition at temperatures not far below the Ohmic regime, scaling well into the Ohmic region. Thus at least over the lower ranges of the Ohmic regime the temperature dependence is of the form $|T-T_t|^{(z+2-d)}$ rather than the activated behavior predicted by Anderson and Kim.[1] The temperature dependences obtained by the use of the values of T_t, and z from our scaling analysis are shown as solid lines in Fig. 9. It is seen that the data follow this dependence extremely well over a range of

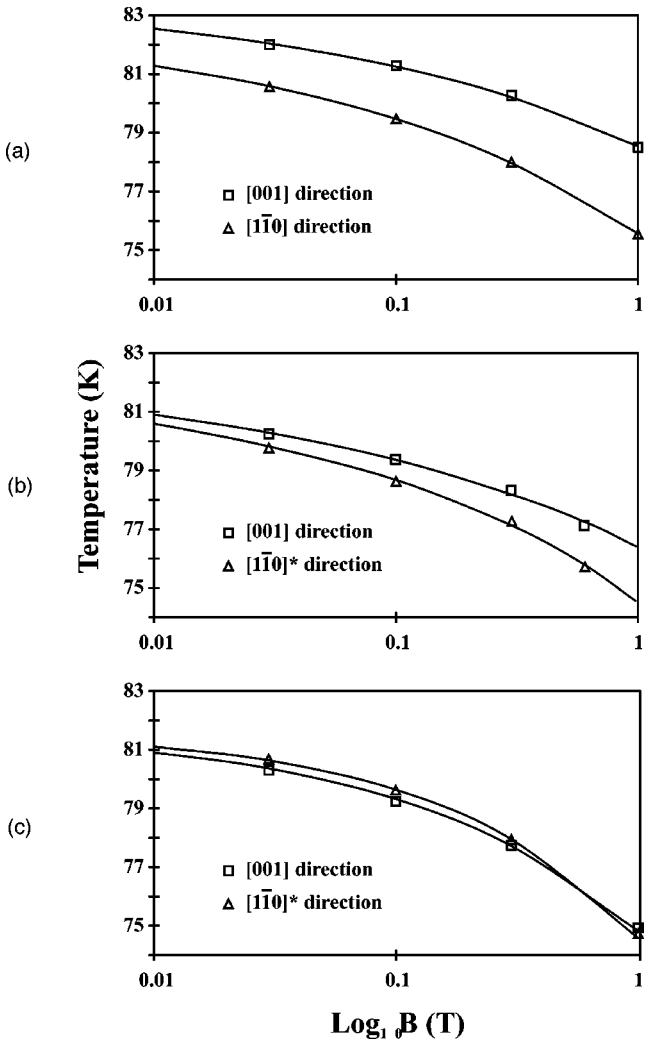

FIG. 8. The phase transition temperature, T_t, as a function of magnetic field for the two transport directions in (a) film 24, 0°, (b) film 34, 3°, and (c) film 41, 5°.

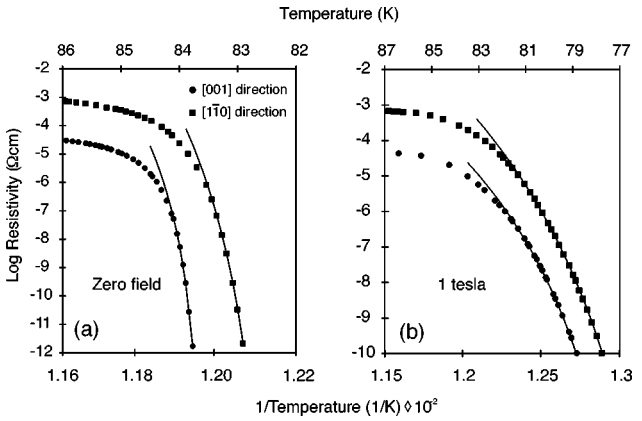

FIG. 9. The Ohmic resistivity as a function of temperature for YBCO film 24 which was grown upon a nominally exact cut substrate. Data are shown for both zero field (a) and a field of 1 T (b), and for the two principle current directions. The solid lines have been obtained by using the scaling parameters.

lower temperatures, but as T_c is approached the experimental resistivities fall below those predicted by scaling.

Figure 9 reveals that the zero-field curves for the two current directions fan out, corresponding to an increase from the normal-state anisotropy which rises with falling temperature. At large fields the superconducting-state anisotropy is more weakly temperature dependent. The variation of the resistive anisotropy with temperature is shown in Fig. 10 for the various film classes and magnetic fields used. The lower-temperature limits to each curve correspond to the onset of nonlinear behavior. T_t, lies typically 1 K below this limit of Ohmic behavior in each case.

Figure 10(a) shows the Ohmic anisotropy for a 0° film. It may be seen that in zero field the anisotropy rises far above the normal-state value as the temperature falls. At higher fields the rise is less pronounced, the Ohmic regime extending to lower temperatures. Figure 10(b) shows the corresponding data for a 3° film. While the anisotropy in zero field rises slightly as the temperature falls, the variation is much less dramatic than in Fig. 10(a). The variation of anisotropy with temperature in finite fields is very small, having much the same magnitude as in the normal state. The results for a 5° film shown in Fig. 10(c) exhibit even less variation with temperature.

The fact that the normal-state anisotropy is preserved through the Ohmic regions of superconducting state in 5° films at all fields and in 3° films at higher fields is remarkable since the temperature range covered includes the critical fluctuation regime, the region of flux flow, and the Ohmic part of the region where critical scaling behavior is observed.

D. Comparative critical current behavior

The critical current has been measured to observe the in-plane anisotropy in the pinning and to identify any weak link behavior. A voltage criterion of 2×10^{-7} V cm^{-1} has been used. In zero field, $J_c[001]$ for film 32 (0° miscut) is 5

TABLE V. Fitting parameters for the function given in the text for the variation of T_t with magnetic field. The midpoint values of the superconducting transition temperature T_c are also given. L refers to [001] transport while H refers to $[1\bar{1}0]$* transport.

Film	Miscut	$T_t(0)$	α	β	T_c
24	0° L	83.6	0.064	0.35	85.5
24	0° H	82.7	0.094	0.37	85.5
34	3° L	82.1	0.076	0.35	84.3
34	3° H	82.0	0.099	0.37	84.3
41	5° L	81.8	0.093	0.48	84.5
41	5° H	81.7	0.094	0.54	84.5

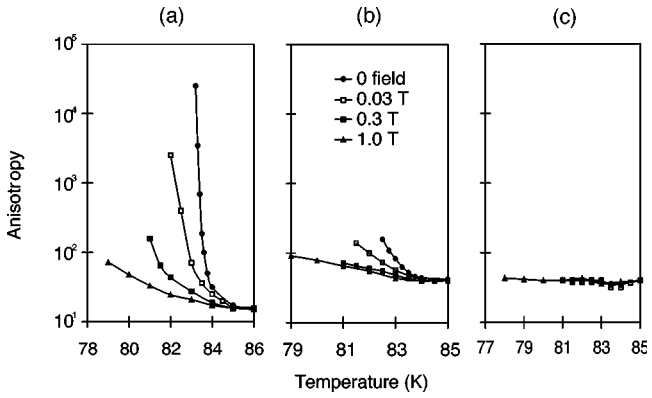

FIG. 10. The Ohmic regime anisotropy as a function of temperature. Data are shown for various classes of the perpendicular magnetic fields used. (a) Data for film 24 (exact cut substrate). (b) Data for film 34 (3° miscut substrate). (c) Data for film 41 (5° miscut substrate).

$\times 10^5$ A cm^{-2} at 75 K and 1.3×10^6 A cm^{-2} at 70 K. The corresponding values for film 34 (3° miscut) and film 41 (5° miscut) are 3×10^5, 8×10^5 and 7×10^5 and 1.3×10^6 A cm^{-2}, respectively. The values for the 0° and 5° films are similar while those for the 3° film are lower by a factor of about 2. At 70 K $J_c[001]$ falls with increasing field initially linearly and reaching half its value by about 0.15 T in the 0° films, by about 0.4 T in the 3° films and by about 0.3 T in the 5° films. This confirms the absence of weak link behavior in any of the films.

The in-plane anisotropy ratios $J_c[001]/J_c[1\bar{1}0]^*$ for the three classes of film at 70 K in applied fields of 0.1 T and 1 T are 6.6 and 6.4 for the 0° films, 6.3 and 8.6 for the 3° films, and 10.0 and 9.1 for the 5° films. There is a general but very slow decline in the anisotropy $J_c[001]/J_c[1\bar{1}0]^*$ with lowering temperature and the anisotropies have a very low dependence upon magnetic field. The ratios for the 0° and 5° films decrease slightly with field; those of the 3° film slightly increase. The changes over the magnetic field range 0–1 T are slight.

The dissipative voltages of the two transport directions for the same driving force on the vortices have a ratio $V[1\bar{1}0]^*/V[001]$, which is of order $(J_c[001]/J_c[1\bar{1}0]^*)^g$, where g is the local gradient of $\log(V)$ versus $\log(I)$. Since g is equal to $(z+1)/2$ at T_t, and increases as the temperature is decreased, we note that the in-plane anisotropy in the dissipation is very large indeed, even when the in-plane anisotropy in J_c is modest.

VII. DISCUSSION

We will restrict our discussions to three topics: the growth of YBCO films with in-plane anisotropy, the anisotropy in the in-plane resistivity in the normal and superconducting states, and the electrical behavior in the critical regime.

We have decribed a two-stage process for reproducibly fabricating (103)/(013) YBCO films. They have an extremely low proportion of other phases such as the (110) phase and very low normal-state resistivities, $\rho_{[001]}$, comparable to the a-axis resistivity of a high-quality YBCO single crystal. The in-plane anisotropy values of the 0° films are in agreement with the meandering-current-path–helical-current-flow model[38] which assumes that the 90° twist boundaries form a negligible impediment to current flow in the [001] direction, while enabling current flow in helical paths along the $[1\bar{1}0]$ direction. The model is supported by the anisotropies observed on very narrow tracks that inhibit circuitous current paths. The normal-state anisotropies of the 3° and 5° films, on the other hand, are consistent with those expected of appropriately tilted good quality single crystals, free of disruptive internal boundaries.

Much may be learned from studying the anisotropy in the electrical properties in the superconducting state. In the superconducting state the dissipation is the result of the movement of vortices, the voltage being directly proportional to the mean vortex flux. Transport current applied in the [001] direction will result in a mean vortex movement in the $[1\bar{1}0]$, ($[1\bar{1}0]^*$ in the case of miscut substrates) direction. In the 0° films vortices moving in this direction will have to cross symmetric tilt boundaries where the superconducting order parameter is suppressed. Transport current applied in the $[1\bar{1}0]$ direction, on the other hand, will result in vortex movement in the [001] direction, along which such pinning processes are not available since the order parameter is not expected to be appreciably suppressed at 90° twist boundaries.[38] This may well explain the increasingly strong anisotropy in the Ohmic behavior found in 0° films as the temperature is lowered through the flux flow regime into the TAFF and TAFC regimes where pinning becomes more and more influential. In the 3° films, where the tilt boundaries are fewer, this anisotropic behavior is less evident, and in the 5° films it is barely detectable.

The fact that the normal-state in-plane anisotropy is preserved through the Ohmic regions of the superconducting state in 5° films at all fields, and in the 3° films for a range of higher fields, is remarkable; the same anisotropy is found in the normal state, in the critical fluctuation regime, through the flux-flow regime where the influence of pinning is weak, through the TAFF region, and into the TAFC region, regimes where pinning is influential (Fig. 10). Only as the temperature passes into the nonlinear regime does the dissipative anisotropy rise towards the very large values which, as we have noted, are found below T_t.

In the superconducting state in-plane anisotropic behavior may result from three basic causes. First, the pinning centers themselves may lead to anisotropy behavior via their shape and arrangement. Second, the vortices themselves may lack axial symmetry as a result of the anisotropic superconducting properties of the medium. In the present 45° tilted structures the vortices will be slightly elliptical in cross section with the major axis along the [001] direction. Such vortices will move more easily along the [001] direction than along the $[1\bar{1}0]$ direction. The third mechanism involves the viscous damping of the vortices. A vortex moves in response to a force F, which is the sum of the Lorentz force, forces due to vortex-vortex and vortex-pin interactions and the forces of thermal excitation. The resulting velocities are limited only by the viscous damping via the realtionship $F=\eta v$, where η is the viscosity. Any anisotropy in η will produce an anisotropy in the dissipation.

Of the three mechanisms for in-plane anisotropy, aniso-

tropic pinning and lack of axial symmetry are ineffective in the flux flow regime. The third mechanism, anisotropy in the viscous damping, is the only one which is expected to be effective in both the flux flow regime, in the TAFF regime, and in the Ohmic portion of the TAFC region. Thus our results appear to require that anisotropy in the viscous damping determine the anisotropy in the flux flow regime of the superconducting state, and that the viscous anisotropy ratio be the inverse of the in-plane anisotropy of the normal-state resistivity. The same viscous anisotropy will also control the anisotropy in the TAFF regime and in the Ohmic portion of the TAFC regime, save in the unlikely event of there being a change in the viscous anisotropy on entering that regime and compensating changes due to the influence of anisotropic pinning and/or anisotropy due to elliptical vortex cross sections.

It might be argued that, since the mean vortex movement is almost transverse to the transport current, if the dissipation results from current through the normal core transverse to the movement, then the anisotropy in the dissipation will be equal to the normal-state anisotropy as we have observed. However, in Bardeen and Stephen's calculation an equal damping is provided by currents near the core.[3] Hao and Clem have extended the calculation to vortices lying along the principal axes of an anisotropic superconductor and show that the damping from currents outside the core involves components of the normal-state resistivity other than that transverse to the vortex movement.[51] The damping is then a superposition of resistivity components; the anisotropy in the damping is less than the anisotropy of the normal-state resistivity. We await a realistic analysis of our own situation where the vortices lie at an angle to the principal crystallographic axes of the material, and the motion of the vortices is varied within the plane of the film.

In all films we have observed transition behavior at a temperature T_t which is typically 2–3 K below T_c for low fields, falling in temperature with increasing field. The quality of the scaling collapses is generally very good indeed. Only close to zero field in the 3° films may it be argued that the assumptions for critical scaling behavior are not met.

A number of the authors[21,22] who have associated the transition with the melting of a vortex glass into a vortex liquid have pointed out that the scaling for a continuous thermodynamic transition should be ''universal.'' Universality implies that scaling should be observed with same critical exponents and master curves for different samples and different sample geometries, for different materials, and for different values of the magnitude and angle of the applied magnetic field. The equivalent critical exponents should be obtained using different measurement techniques. In their extensive work on microtwinned YBCO single crystals Yeh and co-workers lend support to ''universality'' by observing the values $\nu = 0.65 \pm 0.03$, $z = 3.0 \pm 0.3$ over a range of magnetic field and magnetic field angles for ''as-grown'' samples as well as for samples dosed with 3 MeV protons to increase the point defect density.[8–11] However, other workers have obtained different values for the scaling exponents. The exponents obtained from susceptibility measurements[7,52] on YBCO single crystals were found to depend upon the angle of the magnetic field ($\nu = 3.1, z = 3.1, B \| c$; $\nu = 1.6, z = 6.3, B \perp c$). Many of the reported values of the exponents obtained from *c*-axis normal YBCO thin films[12,43,45,53,54] lie in the range $\nu = 1.7 \pm 0.2, z = 5 \pm 1$ for a range of magnetic fields above 0.1–0.5 T. Wöltgens *et al.*[45] report $\nu = 1.7 \pm 0.1$ and $z = 5.85 \pm 0.1$, independent of magnetic field angle; Kötzler *et al.*[52] report $\nu = 1.7 \pm 0.1$ and $z = 5.5 \pm 0.5$ in ac measurements made over ten decades of frequency, again using their results to support universality. Most of these workers have used films which have a thickness of about 300 nm. These exponent values are therefore consistent with those of Sawa *et al.*[14] who report a film thickness dependence of the exponents in which $z \approx 9$ for very thin films, $z \approx 5$ for 300 nm, and $z \approx 4$ for films of 1000 nm thickness. Other work indicates poor scaling or no transition at all in very thin films.[46] Ando *et al.*[15] report low values of ν and high values of z for very narrow tracks ($\nu = 0.7, z = 9.7$, for 0.5 μm; $\nu = 1.2, z = 5.6$ for 5.6 μm). It is very clear that sample geometry affects the exponents. In strained YBCO films grown upon YSZ the exponents change from $\nu = 1.15, z = 8.5$ to $\nu = 1.6, z = 5$ at fields of around 0.1 T.[55]

In *c*-axis normal thin films of the very anisotropic high-temperature superconducting (HTS) thallium compounds values of $\nu = 1.3, z = 7.9$ have been reported for the 1:2:2:3 phase and $\nu = 0.98, z = 6.8$ for the 2:2:2:3 phase, in an analysis[16] based on the plausible assumption that $d = 3$. A report on 2:2:1:2 thallium films shows ν in the range 1.3–1.6 while z steadily increases with magnetic field from $z = 5$ at 0.1 T, through $z = 10$ at 1 T to about $z = 13$ at 5 T, the analysis[17] again being based on $d = 3$. The very high values of the exponent z reported for films of the 2:2:2:3 phase of BSCCO, where $\nu = 0.7$ and $z = 12.5$, have led the authors to change their analysis from $d = 3$ to $d = 2$, yielding $\nu = 1.4$ and $z = 5.6$.[15] Unlike YBCO, the structures of the HTS bismuth and thallium compounds consist of superconducting layers that are very weakly coupled and in some situations these materials may be regarded as two dimensional. However, there are strong theoretical reasons which indicate that a true vortex-glass transition cannot exist in two dimensions.[27] The absence of a vortex-glass transition in ultrathin YBCO films has been demonstrated experimentally by Dekker and Wöltgens.[56]

Many authors have observed scaling, but it is clear that the claim for ''universality'' of the scaling exponents is only valid in a qualified sense. It is certainly true that for a particular sample, or within a group of samples prepared in much the same way, the scaling exponents may be almost independent of the magnitude of the magnetic field over some extended range of field, may have a low dependence upon field angle, and may not vary strongly with sample irradiation. However, the literature also reveals considerable variations with sample, sample geometry, with material, and between single crystals and thin films of nominally the same material. These variations are much larger than the errors in any particular estimate of ν and z.

The present study of scaling behavior is on high-quality thin films with tilted axes. The in-plane anisotropy enables the transition behavior to be probed with different directions of transport current. For the same transport direction we find that ν and z show systematic variations with both film class and magnetic field rather than displaying ''universal'' behavior. The variations of z and ν with transport direction are also greater than the errors in any individual estimate.

Moreover, for the 0° and 3° films differences occur between the values of T_t obtained from the two transport directions for the same sample and the same magnetic field. In the case of the 0° films the differences are considerable, and even in the case of the 3° films the differences for larger fields lie well outside estimates of the experimental errors. This variation of T_t with transport direction strongly correlates with tilt disorder.

The existence of phase transition behavior in zero magnetic fields is also of interest. Some authors are of the opinion that the vortex melting line for YBCO is not expected to extend to zero magnetic field since it folds back close to the boundary of the Meissner phase;[1] in this case some explanation of the phase transition behavior is necessary other than attributing it to a vortex-glass to vortex-liquid transition.

The very high values which we have obtained for the product $z\nu$ are intriguing since they are clearly unphysical if a time scale varying as $|T-T_t|^{-z\nu}$ is involved. Examination of Table II indicates that excellent scaling has been observed for values of $|T-T_t|$ ranging over a decade above T_t and in some cases approaching a range of two decades below T_t. These are lower estimates, which have been obtained by assuming that the lower limit of $|T-T_t|$ is given by the uncertainty in estimating T_t during scaling, rather than from any evidence that scaling has failed close to T_t. Ranges as large as these, together with high values of $z\nu$, appear to imply that scaling behavior occurs over an unphysical time range; $z\nu=16$ implies a range of 20–30 decades. Such a range of voltage is found in Fig. 7.

What can be said about this intriguing situation? It is clear that the current-voltage behavior of all three classes of film exhibits very clean scaling under the algorithms described in Sec. VI B above. The origin of such clean scaling is, however, not at all obvious. The characteristics of a vortex-glass to vortex-liquid transition were discussed by Fisher, Fisher, and Huse[7] but the idea that the current-voltage characteristics should show scaling goes back to the work of Wolf, Gubser, and Imry[57] on thin films. The work of Fisher, Fisher, and Huse is based on an analogy between the putative vortex-glass phase and the scaling theory of short-range spin glasses (Bray and Moore,[58] Fisher and Huse,[59] McMillan[60]). The basic picture is of a state in which the phase degrees of freedom of the pairing field lock into a unique configuration separated from metastable configurations by a hierarchy of free energy barriers whose heights diverge in the thermodynamic limit. The linear conductivity of such a state vanishes, the voltage response to an applied current being nonlinear. The expectation that close to the line of continuous phase transitions between the glass and liquid states the physics is entirely dominated by the divergence of a single correlation length and a single time leads to the scaling which has been described in Sec. IV B.

Superficially this appears to explain the scaling which we have observed, but in fact there are severe problems with the explanation. Although the correlation length exponents that have been extracted from the data are quite plausible, the values of the dynamical exponent are too large to be credible. While one could invoke the existence of anomalous dimensions for the electric field or current density to reduce these values there is a more serious objection.

As has been seen, the anisotropic structure of the 0° and 3° samples has such a strong influence that the characteristic temperature T_t in the scaling depends upon the direction of the current. This is not at all explicable within the above framework which assumes a change in the response of a system to an applied current occurring at an equilibrium transition (with a unique temperature at a given magnetic field).

Giamarchi and Le Doussal[61] have considered the possibility of a moving glass state in which a depinned vortex glass is flowing with a definite average velocity. They find that the vortices flow in static preferred channels and retain ordering in the direction transverse to the average flow; Balents *et al.*[62] have referred to this state as a transverse smectic state. In the presence of a very anisotropic potential it is quite conceivable that such a state would exhibit a nonequilibrium melting transition at a temperature that depends on the current direction. Neither the melting of the moving glass phase nor the details of the depinning transition are well understood at present.

It is, however, not clear that such a transition should exhibit such clean scaling; one might very well expect the critical temperature for this nonequilibrium transition to depend upon the magnitude of the current as well as upon its direction and upon the magnetic field. Clearly the properties of a moving glass close to the depinning threshold and, in particular, the possibility of a sharp nonequilibrium transition are well worth further investigation despite the extreme difficulties of such problems. Whether or not such an investigation could explain the data presented here is less clear but it seems very hard to think of any way in which the direction of the current can affect T_t within any picture based on an equilibrium phase transition.

ACKNOWLEDGMENTS

This work has been supported by the EC under ESPRIT Project No. 8132-WELITTD-HTS, and through a NETWORK program. We are extremely grateful to D. Fuchs and R. Schneider of the Forschungszentrum Karlsruhe, Germany for carrying out detailed XRD measurements on our samples. R.P.C. wishes to thank the EPSRC for financial support.

[1] See, for example, M. Tinkham, *Introduction to Superconductivity*, 2nd ed. (McGraw-Hill, New York, 1996).

[2] G. Blatter, M. V. Feigel'man, V. B. Geshkenbein, A. I. Larkin, and V. M. Vinokur, Rev. Mod. Phys. **66**, 1125 (1994).

[3] J. Bardeen and M. J. Stephen, Phys. Rev. **140**, A1197 (1965).

[4] P. H. Kes, J. Aarts, J. Van den Berg, C. J. van der Beek, and J. A. Mydosh, Supercond. Sci. Technol. **1**, 242 (1989).

[5] P. W. Anderson, Phys. Rev. Lett. **9**, 309 (1962); P. W. Anderson and Y. B. Kim, Rev. Mod. Phys. **36**, 39 (1964).

[6] M. P. A. Fisher, Phys. Rev. Lett. **62**, 1415 (1989).

[7] D. S. Fisher, M. P. A. Fisher, and D. A. Huse, Phys. Rev. B **43**, 130 (1991).

[8] N. C. Yeh, W. Jiang, D. S. Reed, U. Kriplani, F. Holtzberg, M. Konczykowski, C. C. Tsuei, and C. C. Chi, Physica C **200**, 374

(1993).
[9] N. C. Yeh, W. Jiang, D. S. Reed, U. Kriplani, and F. Holtzberg, Phys. Rev. B **47**, 6146 (1993).
[10] W. Jiang, N. C. Yeh, D. S. Reed, U. Kriplani, T. A. Tombrello, A. P. Rice, and F. Holtzberg, Phys. Rev. B **47**, 8308 (1993).
[11] D. S. Reed, N. C. Yeh, W. Jiang, U. Kriplani, D. A. Beam, and F. Holtzberg, Phys. Rev. B **49**, 4384 (1994).
[12] J. Kötzler, G. Nakielski, M. Baumann, R. Behr, F. Georke, and E. H. Brandt, Phys. Rev. B **50**, 3384 (1994).
[13] K. Yamafuji and T. Kiss, Physica C **258**, 197 (1996).
[14] A. Sawa, H. Yamasaki, Y. Mawatari, H. Obara, M. Umeda, and S. Kosaka, Phys. Rev. B **58**, 2868 (1998).
[15] Y. Ando, H. Kubota, and S. Tanaka, Phys. Rev. Lett. **69**, 2851 (1992).
[16] O. B. Hyun, T. Nabatane, S. Koike, H. Suhara, and I. Hirabayashi, Phys. Rev. B **52**, 15 545 (1995).
[17] H. C. Li, J. W. Li, R. L. Wang, B. Yin, Z. X. Zhao, S. L. Yan, L. Fang, and M. S. Si, Physica C **246**, 330 (1995).
[18] P. S. Czerwinka, R. P. Campion, K. Horbelt, P. J. King, S. Misat, S. M. Morley, H-U. Habermeier, and B. Leibold, Physica C (to be published).
[19] S. J. Pennycook, M. F. Chisholm, D. E. Jeson, R. Feentra, S. Zhu, X. Y. Zheng, and D. J. Lowndes, Physica C **202**, 1 (1992).
[20] Z. Trajanovic, C. J. Lobb, M. Rajeswari, I. Takeuchi, C. Kwon, and T. Venkatesan, Phys. Rev. B **56**, 925 (1997).
[21] M. Covington, R. Scheuerer, K. Bloom, and L. H. Greene, Appl. Phys. Lett. **68**, 1717 (1996).
[22] E. Olsson, A. Gupta, M. D. Thouless, A. Segmuller, and D. R. Clarke, Appl. Phys. Lett. **58**, 1682 (1991).
[23] T. Terashima, Y. Bando, K. Iijima, K. Yamamotu, K. Hirata, K. Hayashi, K. Kamigaki, and H. Terauchi, Phys. Rev. Lett. **65**, 2684 (1990).
[24] J. E. Pohl, A. Kirk, P. J. King, J. S. Lees, and W. B. Roys, Supercond. Sci. Technol. **4**, 499 (1991).
[25] C. B. Eom, A. F. Marshall, Y. Suzuki, T. H. Gaballe, B. Boyer, R. F. W. Pease, R. B. van Dover, and J. M. Phillips, Phys. Rev. B **46**, 11 902 (1992).
[26] R. P. Campion, K. Horbelt, P. J. King, S. M. Morley, H-U. Habermeier, and B. Leibold, J. Alloys Compd. **251**, 161 (1997).
[27] H. Lengfellner, S. Zeuner, W. Prettl, and K. F. Renk, Europhys. Lett. **25**, 375 (1994).
[28] M. Matsui, K. Yamamoto, M. Nakajima, T. Shimano, and H. Matsuba, Supercond. Sci. Technol. **5**, S427 (1992).
[29] D. H. Lowndes, X. Y. Zheng, S. Zhu, J. D. Budai, and R. J. Warmack, Appl. Phys. Lett. **61**, 852 (1992).
[30] T. Haage, J. Zegenhagen, J. Q. Li, H-U. Habermeier, M. Cardona, Ch Jooss, R. Warthmann, A. Forkl, and H. Kronmller, Phys. Rev. B **56**, 8404 (1997).
[31] T. Haage, J. Zegenhagen, H-U. Habermeier, and M. Cardona, Phys. Rev. Lett. **80**, 4225 (1997).
[32] J. Tsujino and Y. Shiohara, Physica C **262**, 236 (1996).
[33] M. Guilloux-Viry, C. Thivet, A. Perrin, M. Sergent, M. G. Karkut, C. Rossel, and A. Catana, J. Cryst. Growth. **132**, 396 (1993).
[34] C. Rossel, A. Catana, R. R. Schulz, E. J. Williams, A. Perrin, M. Guilloux-Viry, and C. Thivet, Physica C **223**, 370 (1994).
[35] D. S. Lineham, E. P. Kvam, L. Hou, and M. McElfresh, Supercond. Sci. Technol. **9**, 739 (1996).
[36] S. Poelders, R. Auer, G. Linker, R. Smithey, and R. Schneider, Physica C **247**, 309 (1995).
[37] A. F. Marshall and C. B. Eom, Physica C **207**, 239 (1993).
[38] R. P. Campion, J. R. Fletcher, P. J. King, S. M. Morley, A. Polimeni, and R. G. Ormson, Supercond. Sci. Technol. **11**, 730 (1998).
[39] H. Hilgenkamp, J. Mannhart, and B. Mayer, Phys. Rev. B **53**, 14 586 (1996).
[40] T. A. Friedmann, M. W. Rabin, J. Giapintzakis, J. P. Rice, and D. M. Ginsberg, Phys. Rev. B **42**, 6217 (1990).
[41] J. R. Fletcher, P. J. King, and R. G. Ormson, Phys. Rev. Lett. **79**, 2522 (1997).
[42] M. V. Feigel'man, V. B. Geshkenbein, A. I. Larkin, and V. M. Vinokur, Phys. Rev. Lett. **63**, 2303 (1989).
[43] R. H. Koch, V. Foglietti, W. J. Gallagher, G. Koren, A. Gupta, and M. P. A. Fisher, Phys. Rev. Lett. **63**, 1511 (1989).
[44] P. L. Gammel, L. F. Schneedmeyer, and D. J. Bishop, Phys. Rev. Lett. **66**, 953 (1991).
[45] P. J. M. Wöltgens, C. Dekker, J. Swüste, and H. W. de Wijn, Phys. Rev. B **48**, 16 826 (1993).
[46] P. J. M. Wöltgens, C. Dekker, R. H. Koch, B. W. Hussey, and A. Gupta, Phys. Rev. B **52**, 4536 (1995).
[47] D. R. Nelson and V. M. Vinokur, Phys. Rev. Lett. **68**, 2398 (1992).
[48] W. Jiang, N. C. Yeh, D. S. Reed, U. Kriplani, D. A. Beam, M. Fonczykowski, T. A. Tombrello, and F. Holtzberg, Phys. Rev. Lett. **72**, 550 (1994).
[49] M. Zeise, Phys. Rev. B **53**, 12 422 (1996).
[50] M. Zeise, Phys. Rev. B **55**, 8106 (1997).
[51] Z. Hao and J. R. Clem, IEEE Trans. Magn. **MAG-27**, 1086 (1991).
[52] J. Kötzler, M. Kaufmann, G. Nakoelski, R. Behr, and W. Assmus, Phys. Rev. Lett. **72**, 2081 (1994).
[53] J. Deak, M. McElfresh, R. Muenchausen, S. Foltyn, and R. Dye, Phys. Rev. B **48**, 1337 (1993).
[54] P. J. M. Wöltgens, C. Dekker, S. W. A. Gielkens, and H. W. de Wijn, Physica C **247**, 67 (1995).
[55] T. Nojima, T. Ishida, and Y. Kuwasawa, Physica C **263**, 424 (1996).
[56] C. Dekker and P. J. M. Wöltgens, Phys. Rev. Lett. **69**, 2717 (1992).
[57] S. A. Wolf, D. U. Gubser, and Y. Imry, Phys. Rev. Lett. **42**, 324 (1979).
[58] A. J. Bray and M. Moore, in *The Heidelberg Colloquium on Glassy Dynamics*, Lecture Notes in Physics Vol. 275, edited by J. L. van Hemmen and I. Morgenstern (Springer, Berlin, 1986).
[59] D. S. Fisher and D. A. Huse, Phys. Rev. Lett. **56**, 1601 (1986).
[60] D. L. McMillan, Phys. Rev. B **31**, 340 (1985).
[61] T. Giamarchi and P. Le Doussal, Phys. Rev. Lett. **76**, 3408 (1996).
[62] L. Balents, M. C. Marchetti, and L. Radzihovshy, Phys. Rev. B **57**, 7705 (1988).